

GT2011-46266

**VALIDATION AND ANALYSIS OF NUMERICAL RESULTS FOR A TWO-PASS
TRAPEZOIDAL CHANNEL WITH DIFFERENT COOLING CONFIGURATIONS OF
TRAILING EDGE**

Waseem Siddique

Department of Energy Technology
Royal Institute of Technology (KTH)
Stockholm, Sweden.

Igor V. Shevchuk

MBtech Group GmbH & Co. KGaA,
Salierstr. 38, 70736 Fellbach-Schmiden, Germany

Lamyaa A. El-Gabry*

Mechanical Engineering Department
The American University in Cairo
New Cairo, Egypt.

Torsten H. Fransson

Department of Energy Technology
Royal Institute of Technology (KTH)
Stockholm, Sweden.

*Research Fellow at Department of Energy
Technology
Royal Institute of Technology (KTH)
Stockholm, Sweden.

ABSTRACT

High inlet temperatures in a gas turbine lead to an increase in the thermal efficiency of the gas turbine. This results in the requirement of cooling of gas turbine blades/vanes. Internal cooling of the gas turbine blade/vanes with the help of two-pass channels is one of the effective methods to reduce the metal temperatures. Especially the trailing edge of a turbine vane is a critical area, where effective cooling is required. The trailing edge can be modeled as a trapezoidal channel. This paper describes the numerical validation of the heat transfer and pressure drop in a trapezoidal channel with and without orthogonal ribs at the bottom surface. A new concept of ribbed trailing edge has been introduced in this paper which presents a numerical study of several trailing edge cooling configurations based on the placement of ribs at different walls. The baseline geometries are two-pass trapezoidal channels with and without orthogonal ribs at the bottom surface of the channel. Ribs induce secondary flow which results in enhancement of heat transfer therefore for enhancement of heat transfer at the trailing edge, ribs are placed at the trailing edge surface in three

different configurations: first without ribs at the bottom surface, then ribs at trailing edge surface in-line with the ribs at bottom surface and finally staggered ribs. Heat transfer and pressure drop is calculated at Reynolds number equal to 9400 for all configurations. Different turbulent models are used for the validation of the numerical results. For the smooth channel low-Re $k-\epsilon$ model, realizable $k-\epsilon$ model, the RNG $k-\omega$ model, low-Re $k-\omega$ model and SST $k-\omega$ models are compared, whereas for ribbed channel low-Re $k-\epsilon$ model and SST $k-\omega$ models are compared. The results show that the low-Re $k-\epsilon$ model, which predicts the heat transfer in outlet pass of the smooth channels with difference of +7%, underpredicts the heat transfer by -17% in case of ribbed channel compared to experimental data. Using the same turbulence model shows that the height of ribs used in the study is not suitable for inducing secondary flow. Also, the orthogonal rib does not strengthen the secondary flow rotational momentum. The comparison between the new designs for trailing edge shows that if pressure drop is acceptable, staggered arrangement is suitable for the outlet pass heat transfer. For the trailing edge wall, the thermal

performance for ribbed trailing edge only, was found about 8% better than other configurations.

INTRODUCTION

The fact that thermal efficiency of the gas turbine is related directly to the gas entry temperature, has led to operate the gas turbines at elevated temperatures. It is therefore necessary for the first stage vanes and blades to withstand temperatures higher than the melting point of the components. Air from the compressor is fed to the internal channels of the vanes/blades to keep the metal temperatures below the melting point. The channel is usually divided into three parts as leading edge, mid-span and trailing edge sections. The trailing edge region is difficult to cool as it is narrow and has very little space for coolant to flow. The treatment is difficult not only due to heat transfer problems but also due to the aerodynamic losses. The aerodynamic losses associated with the trailing edge enforce the requirement of a narrow and smooth trailing edge. Therefore a compromise is forced between blade cooling and aerodynamic losses.

The conventional method of cooling the trailing edge is to provide the trailing edge slots, where from, the coolant leaves the blade. This ejected coolant mixes with the gas path and not only reduce the temperature of main flow but also adds to the aerodynamic losses. On other hand the internal cooling for the trailing edge has limitations like small flow area. A better design of internal cooling of trailing edge is therefore required. In case of internal cooling, the coolant is fed to the two-pass channels which are cast in the blade. The phenomenon like impingement, flow separation and recirculation are characterized by the flow in such channels. The heat transfer enhancement is obtained on expense of the pressure drop. An acceptable two-pass channel requires optimized heat transfer enhancement and pressure drop. The literature survey has shown that these are modeled as rectangular or trapezoidal channels depending upon their location in the blade. Metzger et al. [1] varied the divider location and the gap at the 180° turn in a two-pass smooth rectangular channel and studied forced convection. They observed a non-uniform enhancement of heat transfer at the bend region due to flow characteristics at the bend. Park et al. [2] studied the effect of sharp turning flows in a two-pass square channel and found very large spanwise variation in heat transfer at the turn and upstream of the outlet pass. Han et al. [3] and Liou et al. [4] showed that heat transfer enhances in a two-pass channel after the turn and this is due to the secondary flow generated by the centrifugal force at the turn. Many researchers [5, 6, 7, 8, and 9] have studied the effect of channel aspect ratio on heat transfer characteristics. They concluded that heat transfer and pressure drop is influenced by the aspect ratio of channel. It was found that the pressure drop in a wide channel is more than the narrow channel.

The two-pass channels are turbulated with ribs to enhance heat transfer. This leads to increase in pressure drop as well. There have been many fundamental studies to understand the heat transfer enhancement phenomena by the flow separation caused by ribs. Han [10, 11] studied the effect of rib pitch to rib

height ratios (P/e) in stationary channels of different aspect ratios and found that a rib pitch to rib height ratio of 10 is optimum for heat transfer in these channels. Chandra et al. [12] showed that increase in number of ribbed wall reduces the heat transfer performance. Wright et al. [13] studied the thermal performance of three different types of ribs (45° angled, V- and W-shaped) in a high aspect ratio ($W/H = 4:1$) channel with Reynolds number varied from 10,000 to 40,000. They found that W-shaped ribs performed better than the other two types of ribs.

The shape of the trailing edge is such that it can be modeled as the trapezoidal channel. Taslim et al. [14] modeled the trailing edge as trapezoidal channel and studied the effect of bleed holes and tapered ribs on the heat transfer and pressure drop. Taslim et al. [15] found that in a trapezoidal channel, half-length ribs on two opposite walls enhance the heat transfer on the two walls with full-length ribs. Moon et al. [16] studied the local distributions of the heat transfer coefficient on all of the walls at the turn of a smooth two-pass channel with a trapezoidal cross section for various rates of airflow through the channel. The heat transfer was found higher at the turn and the outlet pass. Lowest flow rate resulted in highest heat transfer due to turn. Lee et al. [17] used naphthalene sublimation technique to study the heat (mass) transfer distribution in a two-pass trapezoidal channel with 180° turn. The results were obtained over a range of Reynolds number for the channel with smooth walls and with ribs on one wall and on two opposite walls. They found that for all cases, the average heat transfer was higher on the downstream of the turn compared to that on the upstream of the turn. Also, the shape of the local heat transfer distribution was found unaffected by the variation in flow rates.

The trapezoidal shape of the cross-section of two-pass channels results in differences in the 3D fluid flow and heat transfer patterns in them as compared to the square or rectangular two-pass channels. Cravero et al. [18] analyzed the flow field and heat transfer in a three-pass trapezoidal channel and showed that the geometry of the channel has strong influence on flow field especially at the regions of flow separation and recirculation. Taslim et al. [19] investigated trapezoidal cooling channels and showed that the trapezoidal channel has higher thermal performance compared to the square channel. It was concluded that the stronger interaction of the adjacent walls results in the increased heat transfer of the trapezoidal duct. Ekkad et al. [20] and Murata et al. [21] investigated heat transfer in straight and tapered (from hub-to-tip) two-pass ribbed channels. They found that at low Reynolds number the heat transfer augmentation in the inlet pass is comparable in both cases, but at high Reynolds numbers the acceleration effect in the tapered channel leads to higher heat transfer as compared to the straight channel. At the outlet pass the heat transfer was found comparable. Kiml et al. [22] studied the rib-induced secondary flow structure inside a trapezoidal channel with rib height proportional to the channel cross-section (proportional ribs) and constant height ribs (non-proportional ribs) at four rib inclinations i.e., 90°, 75°, 60° and

45°. They concluded that the proportional ribs offer less pressure losses, but they deteriorate the strength of the secondary flow rotational momentum as a result of wider space for the air flow between the rib and the opposite wall. Also, the strength of the secondary flow rotational momentum increases with change of rib inclination from 90° to 45°.

There have been many numerical studies performed to analyze the flow and heat transfer in the two-pass channel with 180° bend. Lucci et al. [23] studied the performance of k - ϵ , k - ω , and RSM (Reynolds Stress Model) in the computation of the turbulent flow in a two-pass smooth channel. For the Reynolds number 100,000, all the three models showed similar results. Su et al. [24] applied the RANS (Reynolds Averaged Navier Stokes) approach in combination with a near wall, second moment turbulence closure to validate experiments performed at $Re=100000$. Pape et al. [25] successfully modeled a two-pass channel with 180° bend and 45° ribs at $Re=100000$, using the realizable version of k - ϵ model with enhanced wall treatment. Shevchuk et al. [26] used the same model for a varying aspect ratio two-pass channel. The inlet channel aspect ratio (W/H) was 1:2, while for the outlet channel it was 1:1. The channels were roughened with 45° ribs and connected together with 180° bend. The simulations were performed for $Re=100000$. They found the model to be effective and time efficient for high Reynolds number flows. To get more accurate results, advanced numerical methods like LES (Large Eddy Simulation) and DES (Detached Eddy Simulation) were used by Sewall et al. [27] and Viswanathan et al. [28]. They concluded that due to computational economy, it is more practical to use RANS methods based on turbulence models to study heat transfer in the convective cooling channel.

In the present study, three different configurations of two-pass trapezoidal channels have been studied keeping the trailing edge as the focus. Table 1 shows the details of the three configurations.

Table 1: The three configurations for augmented heat transfer at trailing edge.

Case A	Ribs on trailing edge only
Case B	Inline ribs on trailing edge and bottom wall of the outlet pass
Case C	The staggered arrangement of ribs at trailing edge and the bottom wall of the outlet pass

The purpose of the study is to analyze the effect of placing ribs at the trailing edge on heat transfer and pressure drop in the channel for the three configurations. The results of this study should help the gas turbine designers to improve the thermal performance of the gas turbine.

NOMENCLATURE

C specific heat, [J/kg K]
D diameter, [mm]

e rib height [mm]
f friction factor
h heat transfer coefficient, [W/ (m² K)]
H height of channel, [mm]
k thermal conductivity of the fluid, [W/ (m K)]
L streamwise distance between locations of the pressure stations in the channels [mm]
m mass flow rate [kg/s]
Nu Nusselt number, ($h D_h/k$)
p pressure, [N/m²]
P pitch [mm]
Pe perimeter [mm]
Pr Prandtl number, ($C_p \mu/k$)
Re Reynolds number, ($\rho V D_h/\mu$)
V velocity, [m/s]
W width, [mm]

Greek symbols

Δ difference
 ρ density, [kg /m³]
 μ dynamic viscosity, [Pa·s]

DESCRIPTION OF PHYSICAL MODEL

Three designs for augmented heat transfer at trailing edge of the gas turbine blade have been analyzed. Figure 1 shows the schematic of the geometrical model of these designs. The basic geometric parameters are the same as used by Lee et al. [17]. A 571.19 mm long inlet pas is connected to an outlet pass with 180° bend. The divider-to-tip wall distance is equal to the width of the inlet channel ($W = 38.1$ mm), while the thickness of the divider wall is 19.1 mm. The outlet pass extended after the last rib to avoid reverse flow effects is 305 mm long. The maximum height of the inlet pass (H_1) is 76.2 mm while the minimum height of the outlet pass (H_2) is 38.1 mm. This makes the angle between the top and bottom wall equal to 21.8 deg. The ribs, which are orthogonal to the flow direction, are placed at a distance of 305 mm from the inlet. The square cross-sectioned ribs have height $e = 3.2$ mm. The pitch-to-rib height distance (P/e) is equal to 12.

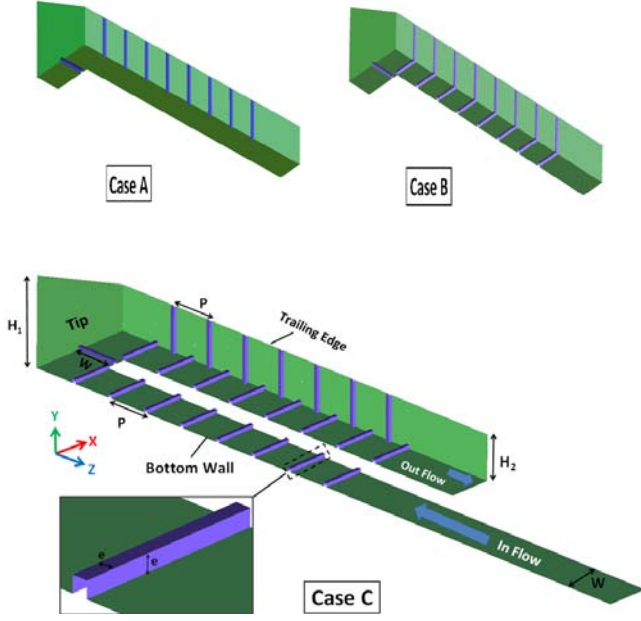


Fig 1. Schematic view of the three designs for augmented heat transfer at trailing edge.

All the three cases have similar geometric configuration at inlet pass, therefore in Fig. 1 inlet pass is shown only in one case. In case A, there are no ribs at the bottom surface and the trailing edge is provided with ribs with same dimensions as those at the inlet pass. Case B, have ribs at both bottom as well as at the trailing edge. The ribs at the bottom wall are inline with the ribs at trailing edge. A staggered arrangement of ribs at outlet pass has been analyzed in case C.

COMPUTATIONAL DETAILS

OVERVIEW

To create geometries and meshes, ANSYS ICEM CFD was used. ANSYS FLUENT was used to solve the numerical problem. As the flow in the two-pass ribbed channels experience phenomenon like flow mixing, correct prediction of the flow field and heat transfer depends on the choice of turbulence model used. Large Eddy Simulation (LES) and Direct Numerical Simulation (DNS) not only require very refined mesh but also is time consuming. This makes these unpopular in terms of computational cost economics. Reynolds averaging of the Navier-Stokes (RANS) equations are thus an acceptable method if the choice of turbulent model is made correctly. Lee et al. [17] performed experiments to study heat transfer distribution in a two-pass trapezoidal channel. For validation of numerical results, the experimental results by Lee et al [29] for smooth channel and a channel with ribs at bottom wall, with flow inlet at larger cross-section were selected. Five different turbulence models provided by FLUENT were tested. These include three $k-\epsilon$ models (low-Re $k-\epsilon$ model, RNG $k-\epsilon$ model and realizable $k-\epsilon$ model) and two $k-\omega$ models (low-Re $k-\omega$ model and SST $k-\omega$ model). These models are known to

perform well in flows where separation and recirculation is present. To model the near-wall region, enhanced wall treatment was used. The enhanced wall treatment combines the two-layer model with enhanced wall functions. The y^+ value near the wall should be close to 1 but values less than 4 to 5 are also acceptable [24]. In all cases, the near-wall regions were meshed such that the y^+ value remain in the range of 1 to 2. The values of the Nusselt number at the bottom wall were monitored and the convergence was assumed when these values cease to change.

PARAMETER DEFINITIONS

The Reynolds number chosen for the current study is defined as

$$Re = \frac{\rho V D_h}{\mu} = \frac{4\dot{m}}{\mu Pe} \quad (1)$$

where D_h and Pe are the hydraulic diameter and the perimeter of the rectangular flow cross-section between the divider wall and the tip wall.

The channel has been divided into a number of sections. As suggested by Shevchuk et al. [21], bulk temperature of each section is used as reference temperature to calculate the heat transfer coefficient at walls of the respective section. To calculate Nusselt number, D_h is used as the reference length. Dittus-Boelter correlation, defined in Eq. 2 has been used to normalize the heat transfer results.

$$Nu_o = 0.023 Re^{0.8} Pr^{0.4} \quad (2)$$

The pressure drop results are presented in terms of the friction factor, which is defined as

$$f = 2\rho \left(\frac{\Delta p}{L} \right) \left(\frac{A_c}{\dot{m}} \right)^2 D_h \quad (3)$$

where Δp is the pressure drop across the turn and is defined as the pressure difference between the static pressures at two streamwise stations near the turn at a distance of 438 mm from the inlet and exit respectively; L is the streamwise distance between the locations of the pressure stations along the centerline and is equal to 362 mm; A_c is the cross-sectional area at the turn of the channel. The friction factor is normalized by the friction factor for fully developed turbulent flow in a smooth channel, which is defined as

$$f_o = [0.790 \ln(Re) - 1.64]^{-2} \quad (4)$$

BOUNDARY CONDITIONS

All the calculations were done at the Reynolds number equal to 9400, which is defined at the turn of the channel. The mass flow rate calculated from Eq. 1 was imposed at the inlet to the channel. In their experiments Lee et al. [17] used naphthalene sublimation technique to measure mass transfer

and then used analogy to estimate heat transfer taking into account the fact that the constant temperature wall boundary condition is analogous to the constant wall concentration of naphthalene in the experiments. The wall was considered to be at 350°C and the fluid inlet temperature was selected to be 310°C. Mass flow rate was calculated based on the Reynolds number at the bend and was used as the inlet boundary condition. For outlet-pass the length was selected equal to the length on which experimental data was taken and an extension equal to twice the hydraulic diameter of the bend region was introduced to take care of reverse flow. Outflow boundary condition was imposed at the outlet.

GRID INDEPENDENCE

ANSYS ICEM is used to generate structured meshes. Figure 2 shows a section of the three grids used for grid independence study of the most complex case i.e., the staggered ribbed channel.

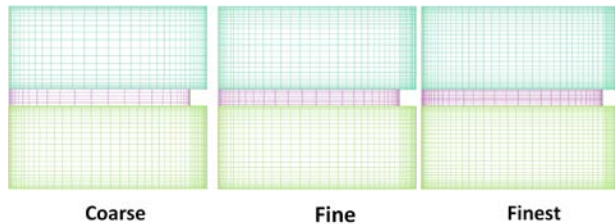


Fig 2. Three grid used for grid independence study.

The three grids namely coarse, fine and finest represent grid sizes equal to 1.9 million, 3.1 million and 4.82 million cells respectively. The near-wall mesh was kept constant in all three cases so that y^+ immediately near the wall was maintained close to unity, and the growth from the wall is at a ratio of 1.2. Area averaged Nusselt numbers at different segments of the channels were compared for the three grids. The detail of these segments is in the next section. A maximum of 1.85 % deviation in the area averaged Nusselt number was found to result from the use of the coarsest and finest meshes. To keep the balance between numerical accuracy and computational economy, coarse grid was selected for further analysis. The same meshing strategy was adopted for the other channels too.

MODEL VALIDATION

Lee et al. [17] performed experiments to study the heat transfer in a trapezoidal channel. The results for the Nusselt number in the smooth channel and the channel with ribs at the bottom wall at the Reynolds number of 9400 have been selected for validation of our numerical model. For the smooth channel, three $k-\epsilon$ models (low-Re $k-\epsilon$ model, RNG $k-\epsilon$ model and realizable $k-\epsilon$ model) and two $k-\omega$ models (low-Re $k-\omega$ model and SST $k-\omega$ model) were evaluated. All these turbulence models and their empirical constants were used as they are implemented in the FLUENT software. The channel was divided into 16 segments by Lee et al. [17]. For validation

purposes, the same segment numbers were used as by Lee et al. [17] and are shown in Fig 3.

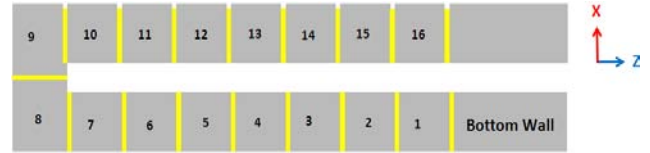


Fig 3. Segment numbers at the bottom wall of the channel.

Figure 4 shows the comparison of $k-\epsilon$ models with experimental results for the smooth channel. All these models underpredict the Nusselt numbers at the inlet pass (till section 7) and bend region (8-9) with the difference of about -10 to -24%. At the outlet pass (10-16) low-Re $k-\epsilon$ model predicts better than the other models with an average difference of about +7%.

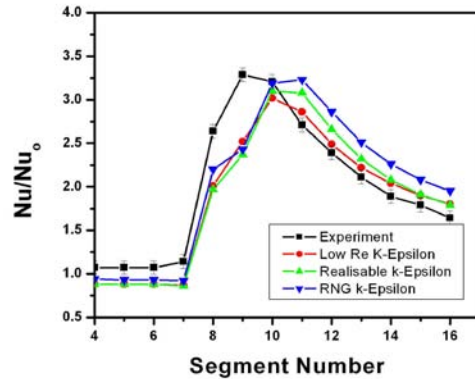


Fig 4. Comparison of numerical results from $k-\epsilon$ models and experimental data for the smooth channel

Figure 5 shows the comparison of two $k-\omega$ models with experimental data for the smooth channel. Both versions of the model predict the same trends with almost similar difference ranges. At the inlet the average difference was about -16% for both cases. At the bend, SST $k-\omega$ model performs better with difference of -12% in contrast to the low-Re $k-\omega$ model, which resulted in difference of about -20%. At the bend, the average difference was found minimum in case of the SST $k-\omega$ model that was -15% in comparison with -18% with the low-Re $k-\omega$ model.

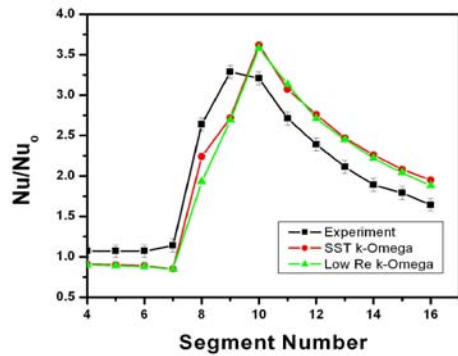


Fig 5. Comparison of numerical results from k- ω models and experimental data for the smooth channel

One turbulence model with the least differences in prediction of heat transfer in the two-pass smooth trapezoidal channel was selected from each of the two groups (k- ϵ and k- ω). Low Re k- ϵ model and SST k- ω model were selected to predict heat transfer in the ribbed two-pass trapezoidal channel with geometrical configurations proposed by Lee et al. [17]. Figure 6 shows the comparison of these two models with experiments for the ribbed channel. SST k- ω model performs the worst and underpredicts Nusselt numbers in the inlet pass with an average difference of about -60% in contrast to low-Re k- ϵ model which performs better with an average difference of -34%. At the inlet the flow was not fully developed, therefore this under-prediction may have resulted from the fact that the two-equation models are suitable for fully developed turbulent flows. At the bend, the SST k- ω model performs better as it is known to be. The average difference at the bend with this model was found to be about -3% in comparison with -9% by the low-Re k- ϵ model. Also, experiments found the peak of the Nusselt number upstream of the outlet pass (segment 10), which was captured by both the models though in magnitude low-Re k- ϵ model was found much closer to the experimental value. The experiment also showed that the peak value remained constant in the subsequent segment, however both turbulence models failed to capture that. In the outlet pass, the average difference resulted from use of the low-Re k- ϵ model was approximately -17%, whilst the SST k- ω model entailed -33%.

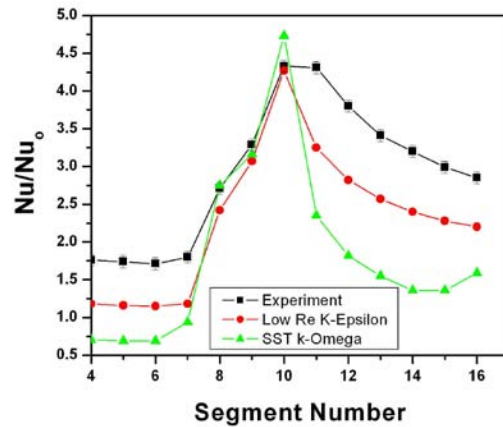


Fig 6. Comparison of numerical results from the low-Re k- ϵ model and SST k- ω model with experimental data for the ribbed channel

Lee et al. [17] calculated pressure losses in the form of the friction factor ratio defined in Eq. 3 and 4. Table 2 presents the experimental and numerical results for both smooth and ribbed channels.

Table 2: Pressure losses in the smooth and ribbed trapezoidal channels.

	f/f_o (Exp)	f/f_o (CFD)	Difference
Smooth	9.3	11.7	+25 %
Ribbed	13.7	13.5	-1.5%

The aim of the study is to evaluate different configurations of the trailing edge, therefore more emphasis is made on matching of numerical predictions with experimental data at the outlet pass. The experimental data has an uncertainty of about $\pm 8\%$ in the Nusselt number and $\pm 7.8\%$ in the friction factor. The predictions by the low-Re k- ϵ turbulence model are accepted for the further analysis of the other configurations of the two-pass channel as it has the minimum difference from experimental data in the outlet pass.

RESULTS AND DISCUSSION

In this section the results for heat transfer and pressure drop in different two-pass trapezoidal channels are presented. Figure 7 to 11 show the Nusselt number distributions normalized with the Nusselt number obtained by the Dittus-Boelter correlation (Eq. 2) on the bottom wall, tip wall and trailing edge of the smooth channel; ribbed bottom wall, ribbed trailing edge only; ribbed bottom wall and trailing edge (inline) and ribbed bottom wall and trailing edge (staggered) of the ribbed channel, respectively.

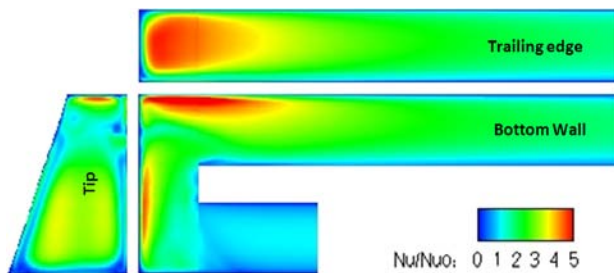


Fig 7. Contours of Nu/Nu_0 for the two-pass smooth trapezoidal channel

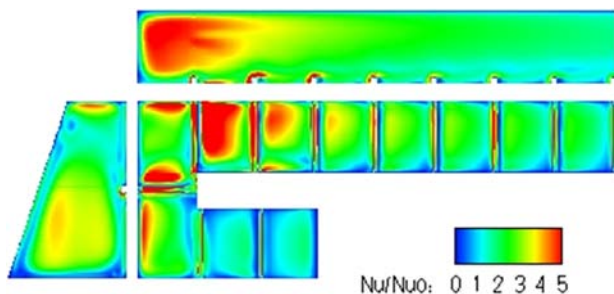


Fig 8. Contours of Nu/Nu_0 for the two-pass ribbed trapezoidal channel

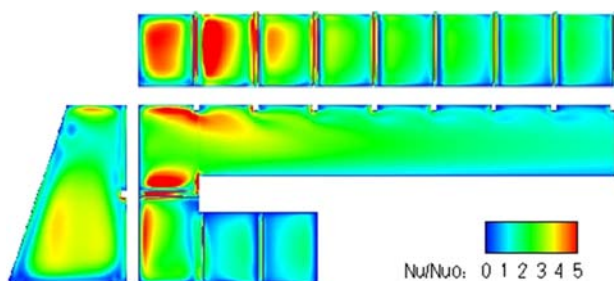


Fig 9. Contours of Nu/Nu_0 for the two-pass trapezoidal channel with the ribbed trailing edge (Case A)

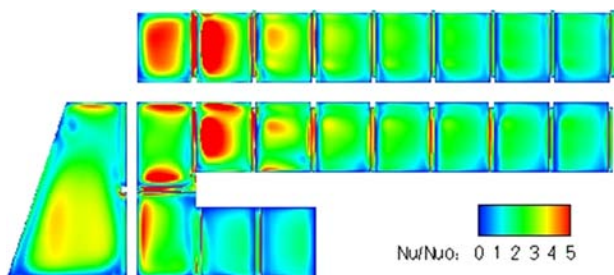


Fig 10. Contours of Nu/Nu_0 for the two-pass trapezoidal channel with ribs on the bottom wall as well as on the trailing edge with inline arrangement (Case B)

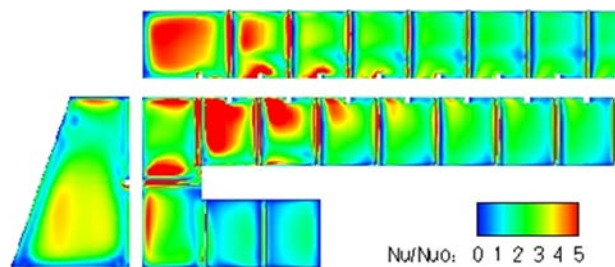


Fig 11. Contours of Nu/Nu_0 for the two-pass trapezoidal channel with ribs on the bottom wall as well as on the trailing edge with staggered arrangement (Case C)

In a smooth channel, fluid impinges on the tip wall that results in a high heat transfer region. The turn at the bend creates secondary flow that causes a high heat transfer spot at the bottom wall in the bend region. A high heat transfer region at the trailing edge wall attached to the bend region is the result of impingement onto the trailing edge wall. Similarly, a region of high heat transfer is observed at the bottom wall upstream of the outlet pass. Further downstream, the effect of bend on flow reduced, and more uniformly distributed heat transfer regions are observed at the bottom wall and trailing edge.

For a channel with ribs on the bottom wall only, the impinging effect is enhanced at the tip wall part close to the inlet pass (Fig. 8 to 11). The bottom wall in the bend region is supplied with ribs. Upstream of this rib, heat transfer is enhanced at the bend bottom near the tip wall, and reduced over the rest of this region downstream of the inlet pass. This reduction in heat transfer is caused by the presence of ribs in the inlet pass. At the bend bottom, the presence of a rib results in the ribbed induced secondary flow that interacts with the bend induced secondary flow (Dean vortices). This interaction appears to be favorable for enhancing heat transfer in the bend. The presence of ribs on the bottom wall of the outlet pass not only enhances heat transfer on the bottom wall itself, but also on the trailing edge wall. In the outlet pass downstream of the bend region, the rib induced secondary flows starts to counteract with the Dean vortices and reduce the impingement effect on the bottom wall. Also, low heat transfer regions start to appear in the outlet pass upstream of the ribs because of the local flow deceleration.

For the geometry shown as Case A in Fig. 1, the channel has ribs only on the trailing edge wall and no ribs on the bottom in the outlet pass. In the bend and the inlet pass, the local heat transfer distribution depicted in Fig. 9 is practically the same as that for a channel with the ribbed bottom wall given in Fig. 8. Qualitatively the effect of ribs on the trailing edge heat transfer in Fig. 9 looks similar to the effect of ribs on the bottom wall heat transfer in Fig. 8.

The inline arrangement of ribs on the bottom and the trailing edge (Case B) results in the cumulative effect in the bend and after the first rib in the outlet pass (Fig. 10). After the second rib, heat transfer drastically reduces, because ribs

destroy bend induced Dean vortices, which would otherwise favor heat transfer enhancement. The comparison between Fig. 10 and 11 shows that there is more enhancement on the bottom wall in case of staggered arrangement but on the trailing edge this arrangement results in low heat transfer regions after the second rib.

To provide an overall measure of enhancement, area averaged Nusselt numbers were calculated for all walls in the outlet pass, bend and tip wall of all the channels. Table 3 presents these results, whereas for the outlet pass and the bend, the area averaging has been taken for the walls including ribs as well as without ribs, which is helpful in separating the enhancement due to increase in the heat transfer area and that due to the ribbed induced secondary flow. The results show that for the outlet pass there is total enhancement of 24% in the Nusselt number in for Case C compared to that of a smooth channel, if ribs are taken into consideration. If the rib area is excluded, this enhancement is about 12%. This shows the share of enhancement due to ribbed induced secondary flow.

Table 3: Area averaged Nu/Nu_0 for different regions of the trapezoidal channels

	Nu_{out}/Nu_0		Nu_{Bend}/Nu_0		Nu_{Tip}/Nu_0
	With ribs	Without ribs	With ribs	Without ribs	
Smooth	1.99	1.99	2.13	2.13	2.10
Ribbed	2.28	2.15	2.29	2.20	2.16
Case A	2.10	2.01	2.26	2.15	2.17
Case B	2.35	2.16	2.30	2.17	2.18
Case C	2.47	2.23	2.28	2.15	2.19

The presence of ribs acts as obstacle to the flow and increases the pressure losses. Eq. 2 was used to calculate the friction factor that represents the pressure drop across the channels shown in Fig. 1. Eq. 3 was used to normalize the results shown in Table 4. Due to more obstacles, case B results in about 36% higher pressure drop compared to a smooth channel. The staggered arrangement reduces this pressure drop by about 4%.

Table 4: Pressure losses in different trapezoidal channels

	Smooth	Ribbed	Case A	Case B	Case C
f/f_0	10.81	13.84	12.93	17.05	16.31

The presence of ribs may enhance heat transfer, but also involves increased pressure losses. To express how much pressure losses are associated with a certain level of heat transfer, a parameter called thermal performance is calculated defined by Eq. 5.

$$\eta = \frac{Nu/Nu_0}{(f/f_0)^{1/3}} \quad (5)$$

Table 5 presents the thermal performance for the outlet pass and bend (including and excluding the ribs in the area of averaging the Nusselt number) and the tip wall region. The

staggered arrangement of ribs shows best results for the outlet pass with 7% increase in thermal performance, if the rib area is considered. However, thermal performance reduces when ribs are excluded in calculating the area-averaged Nusselt numbers. This shows that the ribs are causing more obstacle than enhancing the heat transfer. Note that this observation is about the average Nusselt numbers. While analyzing the local distribution, shown in Fig. 8-11, it was observed that after rib 1 and 2, there is rib induced secondary flow resulting in enhancement of heat transfer but it weakens later on, which in total cause the ribs to be ineffective in enhancing heat transfer.

Table 5: Thermal performance for different regions of the trapezoidal channels

	η_{out}		η_{Bend}		η_{Tip}
	With ribs	Without ribs	With ribs	Without ribs	
Smooth	0.90	0.90	0.96	0.96	0.95
Ribbed	0.95	0.90	0.95	0.91	0.90
Case A	0.90	0.86	0.96	0.92	0.93
Case B	0.91	0.84	0.89	0.84	0.85
Case C	0.97	0.88	0.90	0.85	0.86

Traditionally the ribs are installed to achieve higher heat transfer resulting from phenomenon like impingement and recirculation induced by the ribs. The ribs configuration along with the flow rate chosen in the present study appears to be non-productive in terms of causing impingement on the surface after the rib. It appears that the most part of heat transfer enhancement with ribs is due to the increase in heat transfer area rather than due to the ribbed induced secondary flow phenomenon. It seems that the ribs are blocking the flow more than resulting in enhancement of heat transfer. Figure 12 shows the velocity magnitudes for case C, at planes at half rib height from the bottom wall and trailing edge. As can be seen, although the flow accelerates on the first several ribs in the outlet pass, the strength of impingement on the walls is rather weak and continues to decrease for the subsequent ribs.

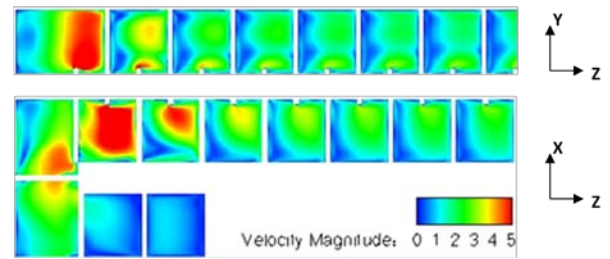


Fig 12. Contours of velocity magnitude for two-pass trapezoidal channel with ribs on the bottom wall as well as on the trailing edge with staggered arrangement (Case C)

The objective of the new designs of trapezoidal channels was to enhance the heat transfer in the trailing edge since that is a critical life limiting region especially when trailing edge slots

are eliminated. Table 6 presents the area averaged Nusselt number normalized with the Nusselt number by the Dittus-Boelter correlation and thermal performance for trailing edge for all cases. This also shows that ribs are not helpful in enhancing heat transfer at the trailing edge, and the smooth wall not only has comparable heat transfer values with other cases but also has the least pressure drop. This results in highest thermal performance for the smooth channel. The results also show that ribs at the trailing edge are enhancing heat transfer due to increase in heat transfer area rather than the ribbed induced secondary flow.

Table 6: Area averaged Nu/Nu_0 and thermal performance for trailing edge of the trapezoidal channels

	Nu/Nu_0		η	
	With ribs	Without ribs	With ribs	Without ribs
Smooth	2.63		1.19	
Ribbed	2.69		1.12	
Case A	2.72	2.46	1.16	1.05
Case B	2.72	2.45	1.06	0.95
Case C	2.49	2.28	0.98	0.90

A rough estimate of the thermal performance for the bottom wall for a smooth and a ribbed bottom wall channel for the region shown in Fig 7 and 8 according to the experimental data is shown in Table 7 along with the numerical results.

Table 7: Thermal performance for the bottom wall of a smooth and a ribbed bottom wall channel

	Experiment	Numerical
Smooth	1.0	0.8
Ribbed	1.1	0.9

The experimental thermal performances found to be better at the bottom wall for the ribbed channel than that of the smooth channel. The numerical results suggest the same though the numerical value is different. This is opposite to what was observed for the trailing edge. It was observed during validations that the Nusselt numbers were underpredicted in the ribbed channel by about 17% whilst for the smooth channel it was overpredicted by about 7% at average, therefore it was concluded that the thermal performance is also underpredicted in case of ribbed channels.

Although the numerical model underpredicts the Nusselt numbers in the ribbed channel, which results in the better thermal performance of the smooth channel, it is worthwhile to compare the three new designs for the enhancement of the trailing edge heat transfer. As shown in Table 4, the heat transfer enhancement is similar in Cases A and B that is higher than that of Case C. But Case B represents higher pressure losses leading to low thermal performance than Case A. So, for the trailing edge perspective, Case A seems to be the better option. But for over all perspective of the outlet pass, Case C is

much better than Cases A and B, if pressure losses are acceptable.

CONCLUSIONS

A numerical study was conducted to evaluate different design for heat transfer enhancement from the trailing edge of the gas turbine blade without ejection holes. The numerical model was validated against the experimental data by Lee et al. [17]. It was found that low-Re $k-\epsilon$ turbulence model predicts heat transfer much better than the other $k-\epsilon$ or $k-\omega$ models in the outlet pass of a two-pass trapezoidal smooth channel. In case of the ribbed channel, this model underpredicts heat transfer by about 17%. There was an increase of 24% in overall heat transfer in the outlet pass for the staggered ribs compared to the smooth channel when rib area was included in the averaging. This reduced to 12% when rib area was excluded from area averaging. The comparison between the Nusselt numbers at the trailing edge of the smooth channel and any other ribbed channel can be misleading as the numerical results overpredicts the Nusselt numbers by about 7% in case of smooth channel while underpredicts the Nusselt numbers by 17% in ribbed channel. But the new trailing edge designs and the ribbed channel can be compared as the prediction is the same for all of these. The comparison shows that with the introduction of ribs, the heat transfer increases at the trailing edge but that is mainly due to increase in the heat transfer area rather than the ribbed induced secondary flow. The comparison of thermal performances indicates that the ribs are causing drop in pressure more than enhancing the heat transfer. The comparison between the new designs for trailing edge heat transfer shows that a channel with ribs on the trailing edge is a better option only due to better thermal performance. If pressure losses are acceptable, the staggered arrangement is a recommended design to be used for the outlet pass heat transfer enhancement. The study shows that the rib height and pitch are important parameters in designing the ribbed channel. A wrong selection may cause resistance to the flow and reduction in heat transfer.

ACKNOWLEDGMENTS

The first author acknowledges the financial support from Higher Education Commission (HEC) of Pakistan and the Division of Heat and Power, Department of Energy Technology, KTH Sweden. The support from Swedish Institute (SI) is also appreciated. The second author acknowledges the financial support from the Division of Heat and Power, Department of Energy Technology, KTH Sweden. The authors are thankful to Dr. Esa Utriainen from SIEMENS Industrial Turbomachinery AB, Finspång, Sweden and Professor Emeritus Torsten Strand, KTH, Stockholm Sweden for valuable discussions. This work was supported by grants of computer time from Parallel Computer Center (PDC) at KTH, Stockholm, Sweden.

REFERENCES

- [1] Metzger, D. E., and Sahm, M. K. 1986, "Heat Transfer around Sharp 180° Turns in Smooth Rectangular Channels," *ASME J. Heat Transfer*, 108, pp. 500–506.
- [2] Park, C. W., and Lau, S. C.; 1998; "Effect of Channel Orientation of Local Heat (Mass) Distributions in a Rotating Two-Pass Square Channel with Smooth Walls"; *ASME J. Heat Transfer*, 120, pp. 624–632.
- [3] Han, J. C., Chandra, P. R., and Lau, S. C., 1988, "Local Heat/Mass Transfer Distributions Around Sharp 180 Deg. Turns in Two-Pass Smooth and Rib- Roughened Channels," *ASME J. of Heat Transfer*, 110, pp. 91–98.
- [4] Liou, T. M., Chen, C. C., and Chen, M. Y., 2003, "Rotating Effect on fluid Flow in Two Smooth Ducts Connected by a 180-degree Bend," *J. of Fluid Engineering*, 125, pp. 138–148.
- [5] Han, J. C., 1988, "Heat Transfer and Friction Characteristics in Rectangular Channels with Rib Turbulators," *ASME J. Heat Transfer*, 110, pp. 321–328.
- [6] Han, J. C., and Park, J. S., 1988, "Developing Heat Transfer in Rectangular Channels with Rib Turbulators," *Int. J. Heat and Mass Transfer*, 31, pp.183–195.
- [7] Park, J. S., Han, J. C., Huang, Y., and OU, S., 1992, "Heat Transfer Performance Comparison of Five Different Rectangular Channels with Parallel Angled Ribs," *Int. J. Heat and Mass Transfer*, 35 (11), pp.2891–2903.
- [8] Astarita, T., and Cardone, G., 2000, "Thermofluidynamic Analysis of the Flow in a Sharp 180deg Turn Channel," *Experimental Thermal and Fluid Science*, 20, pp. 118–200.
- [9] Cai, L., Ota, H., Hirota, M., Nakayama, H., and Fujita, H.; 2004, "Influence of Channel Aspect Ratio on Heat Transfer Characteristics in Sharp-Turn Connected Two-Pass Channels with Inclined Divider Wall," *Experimental Thermal and Fluid Science*, 28 , pp. 513–523.
- [10] Han, J. C., Gliksman, L. R., and Rohsenow, W. M., 1978, "An Investigation of Heat Transfer and Friction for Rib-Roughened Surfaces," *Int. J. Heat Mass Transfer*, 21, pp. 1143–1156.
- [11] Han, J. C., 1984, "Heat Transfer and Friction in Channels with Two opposite Rib-Roughened Walls," *ASME J. Heat Transfer*, 106, pp.774–781.
- [12] Chandra, P. R., Alexander, C. R., and Han, J. C., 2003, "Heat Transfer and Friction Behaviors in Rectangular Channels with Varying Number of Ribbed Walls," *Int. J. Heat and Mass Transfer*, 46, pp. 481–495.
- [13] Wright, L. M., Fu W. L., and Han J. C., 2004, "Thermal Performance of Angled, V-Shaped, and W-Shaped Rib Turbulators in Rotating Rectangular Cooling Channels (AR=4:1)," *Proceedings of the 2004 ASME Turbo Expo (June 14-17, 2008, Vienna, Austria)*, GT2004-54073.
- [14] Taslim, M. E., Li, T., and Spring, S. D., 1995, "Experimental Study of the Effects of Bleed Holes on Heat Transfer and Pressure Drop in Trapezoidal Passages With Tapered Turbulators," *ASME J. Turbomach.*, 117, pp. 281–289.
- [15] Taslim, M. E., Li, T., and Spring, S. D., 1998, "Measurements of Heat Transfer Coefficients and Friction Factors in Passages Rib-Roughened on All Walls," *ASME J. Turbomach.*, 120, pp. 564–570.
- [16] Moon, S. W., Endley, S., and Lau, S. C., 2002, "Local Heat Transfer Distribution in a Two-Pass Trapezoidal Channel With a 180° Turn via the Transient Liquid Crystal Technique," *J. Energy, Heat and Mass Transfer*, 24, pp. 103–121.
- [17] Lee, S. W., Ahn, H. S., Lau, S. C., 2007, "Heat (Mass) Transfer Distribution in a Two-Pass Trapezoidal Channel With a 180° Turn," *ASME J. Heat Transfer*, 129, pp. 1529–1636.
- [18] Cravero, C. , Giusto, C. and Massardo, A.F., 1999, "Fluid Flow and surface Heat Transfer Analysis in a Three-Pass Trapezoidal Blade Cooling Channel," *Aircraft Engineering and Aerospace Technology*, 71, pp. 143–153.
- [19] Taslim, M. E., Li, T., and Spring, S. D., 1997, "Measurements of Heat Transfer Coefficients and Friction Factors in Rib-Roughened Channels Simulating Leading-Edge Cavities of a Modern Turbine Blade", *ASME J. of Turbomachinery*, 119, pp. 601–609.
- [20] Ekkad, S. V., Pamula, G., Shatiniketanam, M., 2000, "Detailed Heat Transfer Measurement Inside Straight and Tapered Two-Pass Channel with Rib Turbulators," *Experimental Thermal and Fluid Science*, 22, pp. 55–163.
- [21] Murata, A., Mochizuki, S., 2004, "Effect of Rib Orientation and Channel Rotation on Turbulent Heat Transfer in a Two-Pass Square Channel with Sharp 180° Turns Investigated by Large Eddy Simulation," *Int. J. Heat and Mass Transfer*, 47, pp. 2599–2618.
- [22] Kiml R., Mochizuki S., Murata A., and Sulitka M., 2003, "Rib-Induced Secondary Flow Structures inside a High Aspect Ratio Trapezoidal Channel - Application to Cooling of Gas Turbine Blade Trailing Edge," *Proceedings of the International Gas Turbine Congress 2003 Tokyo IGTC2003Tokyo TS-078*.
- [23] Lucci, J.M., Amano, R.S., Guntur, K. and 2007, "Turbulent Flow and Heat Transfer in Variable Geometry U-Bend Blade Cooling Passage," *Proceedings of the 2007ASME Turbo Expo (May 14-17, 2007, Montreal, Canada)*, GT2007-27120.
- [24] Su, G., Chen, H. C., Han, J. C., and Heidmann, J. D., 2004, "Computation of Flow and Heat Transfer in Two-Pass Rotating Rectangular Channels (AR=1:1, AR=1:2, AR=1:4) With 45-Deg Angled Ribs by a Reynolds Stress Turbulence Model," *Proceedings of the 2004 ASME Turbo Expo (June 14-17, 2008, Vienna, Austria)* , GT2004-53662.
- [25] Pape, D., Jeanmart, H., von Wolfersdorf, J., and Weigand, B., 2004, "Influence of the 180° Bend Geometry on the Pressure Loss and Heat Transfer in a High Aspect Ratio Rectangular Smooth Channel," *Proceedings of the 2004 ASME Turbo Expo (June 14-17, 2008, Vienna, Austria)*, GT2004-53753.
- [26] Shevchuk, I.V., Jenkins, S.C., Weigand, B., von Wolfersdorf, J., Neumann, S.O., and Schnieder, M.,

- “Validation and Analysis of Numerical Results for a Varying Aspect Ratio Two-Pass Internal Cooling Channel,” *ASME J. Heat Transfer*, 2011, 133 (5), p. 051701
- [27] Sewall, E. A., and Tafti, D. K., 2005, “Large Eddy Simulation of Flow and Heat Transfer in the 180o Bend region of a Stationary Ribbed Gas Turbine Internal Cooling Duct,” *Proceedings of the 2005 ASME Turbo Expo (June 6-9, 2005, Nevada, USA)*, GT2005-68518.
- [28] Viswanathan, A. K., and Tafti, D. K., 2006, “Detached Eddy Simulation of Turbulent Flow and Heat Transfer in a Two-Pass Internal Cooling Duct,” *Int. J. of Heat and Fluid Flow*, 27, pp. 1-20.
- [29] ANSYS FLUENT User’s Guide, Version 12, ANSYS Inc., January 2009.